European Journal of Operational Research 285 (2020) 263–278

Contents lists available at ScienceDirect

European Journal of Operational Research

journal homepage: www.elsevier.com/locate/ejor

Production, Manufacturing, Transportation and Logistics

Increasing electric vehicle adoption through the optimal deployment of fast-charging stations for local and long-distance travel

Miguel F. Anjos[a], Bernard Gendron[b], Martim Joyce-Moniz[a,*]

[a] Polytechnique Montréal & GERAD, Canada
[b] Université de Montréal & CIRRELT, Canada

ARTICLE INFO

Article history:
Received 9 August 2018
Accepted 26 January 2020
Available online 3 February 2020

Keywords:
Transportation
Electric vehicle charging stations
Facility location
Integer programming
Large demand dynamics

ABSTRACT

We present a new strategic multi-period optimization problem for the siting of electric vehicle (EV) charging stations. One main novelty in this problem is that EV adoption over time is influenced by the availability of charging opportunities, as well as by local EV diffusion. Furthermore, to the best of our knowledge, this is the first contribution where the distribution of charging demand is modeled with a combination of node-based - more appropriate for urban or suburban settings - and flow-based approaches - with which we can model the needs of EVs to recharge on intermediary stops on long-haul travels. We propose a mixed-integer linear programming (MILP) formulation for this problem. Our computational experiments show that by simply implementing it in state-of-art MILP solvers, we are unable to obtain feasible solutions for realistically-sized instances. As such, we propose a rolling horizon-based heuristic that efficiently provides provably good solutions to instances based on much larger territories (namely the province of Quebec and the state of California) than those tackled by the methods proposed in the literature for the location of EV charging stations.

1. Introduction

Major reforms to the transportation sector are necessary if humanity is to stymie the advances of climate change. In 2015, this sector was responsible for around a quarter of all the greenhouse gas emissions in Canada (Canada & Change, 2017), U.S. (Agency, 2017b) and Europe (Agency, 2017a). Electric vehicles (EVs) have long been regarded as an auspicious way to curtail the emissions produced by road transportation, as well as to decrease our dependency on limited fossil energy sources. As such, many countries have started setting ambitious targets for future EV adoption (Perwoski, 2017); some are even reportedly planning to ban the sale of internal combustion engine vehicles (ICEVs) altogether, as early as of 2025 (Petroff, 2017). EVs have zero tank-to-wheel emissions, and depending on the electric energy sources, they can also have substantially lower well-to-wheel emissions than those of ICEVs (Woo, Choi, & Ahn, 2017).

There are still, however, important hurdles that must be overcome for mass market adoption of EVs to become a reality. One of them is that, as of 2018, the average purchasing cost of an EV is significantly higher than that of an ICEV, and thus not accessible to a large share of people. For that reason, some countries offer incentives to purchasing EVs, such as rebates, tax exemptions or access to high-occupancy lanes (Tietge, Mock, Lutsey, & Campestrini, 2016). Supply-side policies like the zero-emission vehicle mandate from California and Quebec, which encourage or require automakers to develop and sell EVs, also have the potential to lower prices over the coming years through competition (Melton, Axsen, & Goldberg, 2017).

Despite considerable technological progress, another major obstacle to mass adoption is the limited travel range of EVs (Li, Huang, & Mason, 2016); according to the U.S. Department of Energy, even though some models offer ranges of more than 500 kilometer, the median range was, as of 2017, only 183 kilometer (Energy & of, 2017). In addition, up until recently, this was aggravated by the hours-long charging idle times that first-generations “slow” chargers imposed. Level 1 chargers through a 120V alternating-current (AC) plug, and take around 20 hours to fully charge of a standard battery EV (with a 20–30kWh sized battery). The second generation of chargers, Level 2, charge through 240V AC plugs and reduce the charging time of a full charge to 4 to 6 hours (Guinn, 2017). This is especially cumbersome for someone who does not have charger access at home, and discourages residents of multi-dwelling housing from adopting EVs

* Corresponding author.
E-mail addresses: miguel-f.anjos@polymtl.ca (M.F. Anjos), bernard.gendron@cirrelt.ca (B. Gendron), martim.joyce-moniz@gerad.ca (M. Joyce-Moniz).

https://doi.org/10.1016/j.ejor.2020.01.055
0377-2217/

(Bailey, Miele, & Axsen, 2015). For these same reasons, long intercity travel has also been all but impossible. Level 3 "fast" chargers can now provide an 80% charge in only 20 to 30 minutes, by charging through a 480V direct-current (DC) plug; for that reason, they are also referred to as Fast DC chargers. A wide-reaching network of these fast chargers, publicly available along both people's daily commutes and longer travel itineraries, can overcome the issues of range anxiety and inconvenient waiting times (Carley, Krause, Lane, & Graham, 2013), making EV mass adoption much more plausible.

It is often observed that charging infrastructure is particularly susceptible to the "chicken or egg" dilemma (see, e.g., Chung & Kwon, 2015; Mirhassani & Ebrazi, 2013; Upchurch & Kuby, 2010): the willingness of customers to purchase EVs is dependent on widespread availability of chargers, yet market-driven investments in chargers are unlikely while adoption is low. Thereby, initial investments for such an extensive infrastructure will likely be mostly driven by governments.

Contributions. In this paper, we present a new optimization framework that can help decision makers discern where best to site new EV stations. In this framework, the goal is twofold: (i) effectively cover present charging demands, and (ii) increase EV adoption over a given time horizon, that allow decision makers to reach the ambitious targets mentioned in the beginning of this section. As such, we study a new strategic multi-period optimization problem that incorporates demand dynamics describing how siting decisions made at one period impact the charging demand in the subsequent periods. This follows recent trends in the literature that deal with the aforementioned "chicken or egg" dilemma. The problem we define in this framework differs however from previous ones in two major ways. First, it is, to the best of our knowledge, the only such problem to combine a node-based approach (see, e.g., Cavadas, de Almeida Correia, & Gouveia, 2015; Frade, Ribeiro, Gonçalves, & Antunes, 2011; Tu et al., 2016) and a flow-based approach (see, e.g., Chung & Kwon, 2015; Hosseini & MirHassani, 2015; Kuby & Lim, 2005; Zhang, Kang, & Kwon, 2017) to model the spatial distribution of the EV charging demand (in Section 2 these two approaches are defined in detail, along with an exhaustive literature review). This integration allows decision makers to optimize the siting of EV chargers in territories that include both urban and inter-urban areas. Second, we incorporate within our framework a new demand dynamic that reflects the positive effect in EV adoption growth of charging availability (Zhang et al., 2017) and social influence (see Section 2 for more detail). We propose a mixed-integer linear programming (MILP) formulation for this problem. Extensive computational results reveal that by simply implementing it in the state-of-art MILP solver CPLEX, we are unable to produce good feasible solutions for most realistically-sized problem-instances. Accordingly, we propose a rolling horizon-based primal heuristic that is capable of efficiently creating good feasible solutions. Thereby, the proposed framework can produce provably-good siting plans for much larger territories than previous state-of-art methods. We validate our framework by showing results for instances that represent the province of Quebec in Canada (2363 candidate siting locations) and the state of California in the U.S. (4608 candidate locations).

Layout. This paper is structured as follows. In Section 2 we present a review of the relevant literature, and further explain the main contributions of our work. In Section 3, we formally define the proposed optimization problem, and in Section 4 we describe a MILP formulation that models it. In Section 5, we present the rolling horizon heuristic. In Section 6, we compare the performance of the CPLEX solving the proposed MILP formulation with and without heuristic, by analyzing results from computational experiments on large sized instances. Finally, in Section 7, we draw conclusions, and discuss future research directions.

2. Literature review

In recent years, the question of how to optimally locate new chargers has received a lot of attention in the literature (Ko, Gim, & Guensler, 2017). The optimization problems studied in the literature typically extend general facility location problems, while tackling technical constraints specific to EVs, including their limited range. In these approaches, a finite set of candidate locations is identified a priori, and one must choose in which of them to site charging stations in order to best serve existing or potential demand. To model the spatial distribution of demand, one of two approaches is usually taken: node-based or flow-based (Upchurch & Kuby, 2010).

In the node-based approach, drivers are assigned to one (Frade et al., 2011; Tu et al., 2016) or a few (Cavadas et al., 2015) fixed locations (e.g., place of residence or work), and they are able to recharge their vehicle as long as there is a charger in the vicinity. These models are more appropriate when deployment decisions are limited to an urban or suburban setting, where most drivers usually do not stray too far from their assigned location(s). Nevertheless, they present an obvious limitation: they cannot account for the limited travel range of EVs that is an issue on long-haul travels, as discussed before.

Thereby, most recent contributions have opted for a flow-based approach for modelling charging demand. In this approach, drivers are instead assigned to origin-destination (OD) pairs, and chargers must be deployed, so that they allow the drivers to complete the itinerary without the battery of their cars running out of energy. A seminal flow-based location problem for refueling/recharging stations for range-limited vehicles is the Fuel Refueling Location Problem (FRLP, often referred to as Fuel Refueling Location Model), first proposed by Kuby and Lim (2005) in 2005. The FRLP seeks to locate a fixed number of refueling stations so as to maximize the share of "captured" flow. This problem has since been receiving a lot of attention. One line of research literature proposes different solution methods or alternative formulations to solve the FRLP more efficiently (Capar, Kuby, Leon, & Tsai, 2013; Lim & Kuby, 2010). Other works have studied different variations or extensions of the FRLP. In Li and Huang (2014),Mirhassani and Ebrazi (2013),Wang and Lin (2009),Wang and Lin (2013) and Wang and Wang (2010), a similar problem is tackled, which instead finds a minimum-cost deployment that covers all the demand. In Hosseini and MirHassani (2015),Hosseini, MirHassani, and Hooshmand (2017) and Upchurch, Kuby, and Lim (2009), capacities are imposed that limit how many vehicles can be served by each station. While in the FRLP each OD pair is assigned a single routing path (normally the shortest one), in Hosseini et al. (2017), Huang, Li, and Qian (2015), Kim and Kuby (2012),Kim and Kuby (2013) and Yıldız, Arslan, and Karaşan (2016) so-called deviation paths are allowed; this suggests that drivers are willing, up to a certain extent, to stray from their shortest route to charge their vehicles.

Despite these recent modeling and algorithmic advances, solving realistic instances of the FRLP still poses significant computational challenges, since in the numbers of OD pairs is extremely large. Therefore, past works on the FRLP have focused on intercity siting contexts, where each node in the underlying network represents a large population center. At the same time, they ignore siting decisions within each such center because considering those with the same flow-based approach would predictably make the problem intractable. This simplification might be acceptable for decision makers looking only to serve early adopters of EVs, who often have access to home chargers. Nevertheless, it is expected that many mainstream adopters will not, since a large share of the populations live in multi-dwelling housing within high-density metropolitan areas, and therefore will also need infrastructure along their daily commutes. Decisions should therefore

be taken, simultaneously, for local and long-distance travel. This dual need has been identified in studies on the location of stations of another alternative fuel, hydrogen. In Brey, Carazo, and Brey (2014), stations are located in areas that allow drivers to travel between covered regions. In the California Hydrogen Infrastructure Tool (CHIT) (Board, 2019), existing and potential coverage is analyzed by measuring different socio-demographic factors of each location, as well the traffic volume flowing through it. Finally, in Kuby et al. (2009), the FRLP is solved separately for the state of Florida in the U.S., and then for the metropolitan area of Orlando, Florida, in order to identify a robust set of stations that add infrastructural value at both scales. To the best of our knowledge, however, the optimization problem proposed in this paper is the first to jointly consider both approaches, node-based for intra-city settings, and flow-based for inter-city travels, for EV charging infrastructure siting decisions.

A major challenge to validate the various approaches proposed in the aforementioned papers is the realistic representation of EV charging demand. Node population is often used to estimate charging demand, either directly as in the case of node-based models (Frade et al., 2011), or as a way to calculate OD flow demand (see, e.g., Capar et al., 2013; Upchurch et al., 2009). Alternatively, in Cavadas et al. (2015),Dong, Liu, and Lin (2014) and Wang and Lin (2013), surveys conducted with drivers of all types of vehicles are used to infer data on EV charging demand, and in Shahraki, Cai, Turkay, and Xu (2015), taxi fleets are used as proxies for EV early adopters. We refer the reader to Ko et al. (2017) for a more complete review. Arguably, the most significant limitation of these approaches is not the accuracy of estimations of current EV ownership, but rather that the numbers and geographical distribution of EV ownership will likely change significantly in the coming years and decades.

Therefore, and also because the necessary infrastructure investment is expensive and must be spread over time, it makes sense to consider strategic multi-period deployment plans that take into account the evolution of demand over the next years (Chung & Kwon, 2015; Li et al., 2016; Xie, Liu, Li, Lin, & Huang, 2018). In Chung and Kwon (2015), the FRLP is extended to multiple periods, and the goal is to maximize the total traffic flow. In Li et al. (2016), the objective is instead to minimize the cost of covering all OD trips, and to integrate the changing network topology dynamics of growing EV markets, new OD trips are added to the network from period to period. The formulation in Xie et al. (2018) is also a set-covering one but it allows partial coverage subject to penalty costs. In addition, Xie et al. (2018) recognizes the importance of considering station capacities and proposes a chance-constrained stochastic formulation that models drivers as finding a vacant charger within a certain amount of time with a given probability.

In Chung and Kwon (2015),Li et al. (2016) and Xie et al. (2018), the spatial distribution and the volume of the charging demand changes over time, but is exogenous to the optimization process, i.e., the siting decisions taken at a given period have no impact on the demand in the subsequent periods. Zhang et al. (2017) identify the importance of incorporating the positive effect that charging availability has on the growth of EV adoption within the optimization problem. Therefore, they propose a multi-period extension of the FRLP with capacity constraints and demand dynamics. These dynamics define the rate at which path-specific EV market shares increase from one period to the next as a weighted sum of two factors: i) the natural growth of EV market share (given as an input), and ii) the charging opportunities for that path, relative to the average charging opportunity of the entire network. Following this, the charging demand at each period is defined by a non-linear function, which leads to a mixed-integer nonlinear program (MINLP). The computational experiments presented in Zhang et al. (2017) show that solving the proposed model with a standard MINLP solver quickly becomes impossible as the size of the instances increase. For example, the authors report that they were not able to find a feasible solution within 2 hours for an instance using the Sioux-Falls test network (24 nodes, 38 edges) (LeBlanc, Morlok, & Pierskalla, 1975), with 16 OD pairs and 3 time periods. For this reason, the authors propose to solve the model on a rolling horizon, i.e., optimize decisions for a single period at a time, and fix those decisions when solving the same subproblem for subsequent periods. In this way, no MINLP problem needs to be solved: since the path-specific market shares can be directly calculated based on the decisions already taken for past periods, nonlinearities disappear in the model representing the single-period subproblems. The results in Zhang et al. (2017) suggest that this method is much more effective in producing feasible solutions than the multi-period model. However, it is hard to evaluate the quality of these solutions relative to the optimal ones. Even though the authors are able to show that, for the small-sized Sioux-Falls instances, the quality of the solutions is similar to the ones generated by the MINLP solver, it is unclear how far from optimality the latter are (none are said to be optimal, and no relaxation bounds are reported).

The problem we consider in this paper is similar to the one in Zhang et al. (2017) in that it also considers multiple installation periods, and also incorporates demand dynamics that model the impact that the investment decisions have on EV adoption in future periods. Nevertheless, there are important differences as to how these demand dynamics are defined. In Zhang et al. (2017), the main dynamic impacting the market share growth rate of a given OD pair is the availability of charging opportunities, compared to the average availability in the entire network. While there are early signs that station availability impacts people's decision to purchase an EV (see, e.g., Brownstone, Bunch, & Train, 2000), to the best of our understanding, no evidence is presented in Zhang et al. (2017) as to why they would perceive their charging opportunities as relative to those of others, and not simply according to their own needs. Moreover, while market shares are associated with OD pairs and the objective is to maximize the total flow coverage, the approach in Zhang et al. (2017) only accounts for the charging needs of EV drivers that always travel between the same origin and destination. By contrast, we consider that drivers expect to be able to travel to multiple destinations, and we cover the charging needs of drivers traveling between two locations based on their likelihood to do so. A similar approach was considered in Hong and Kuby (2016), where the authors consider an extension to the FRLP that is motivated by the idea that drivers will only chose to adopt EVs if a critical number of their regular itineraries can be completed.

We define a new demand dynamic to be incorporated in the proposed optimization problem. At each period, and for each urban zone, we first estimate the number of potential new EV adopters as a function of the number of EV owners in the previous period. This dynamic implies that there is a contagion-like effect to EV adoption, where as people see more EVs around, they become more comfortable with the idea of owning one (Plumer, 2016a; Wolf, der, Neumann, & de Haan, 2015). This effect, referred to as "diffusion of innovations" (Rogers, 2003), has been observed in the spread of many technologies, including other green technologies like rooftop solar (Plumer, 2016b). In 2014, an initiative from the U.S. Department of Energy (Everywhere, 2014) saw that employees of workplaces with a charging station were 20 times more likely to drive an EV than the average worker, suggesting that peoples' decision to adopt EVs might also be influenced by their social environment and network. In Wolf et al. (2015), the authors present a realistic agent-based model for the adoption of EVs, that considers the effect of this social influence. Our model imposes no pre-conditions on the shape of the aforementioned growth

function (further on, in Section 6.2, we discuss some possibilities based in real-life data); since the remaining optimization problem is already discrete, we do however approximate it with a piecewise linear function, thereby benefiting from the powerful capabilities of existing MILP solvers. The final determination of how many of these potential customers ultimately decide to purchase an EV is based on the charging opportunities available, both close to their place of residence, and along their more traveled (longer) routes.

3. Problem definition and notation

In this section, we formally define the optimization problem studied in this paper and introduce the notation. Let T be the set of investment periods, and N the set of candidate locations where a charging station might be installed. Much like a conventional gas station can have multiple pumps, an EV *charging station* can have multiple *chargers*. We denote as l_j the number of chargers already sited at location $j \in N$, before the start of the time horizon described by T (it is possible that $l_j = 0$). The installation cost per charger is denoted as c^U, and c^F_j is the one-time cost of opening a charging station in j, including the cost of the land purchase and electrification ($c^F_j = 0$ if $l_j > 0$). Siting decisions are limited by an overall budget B, and a maximum budget per period b^t (in general, $\Sigma_{t \in T} b^t > B$), as well as local bounds e_j that restrict how many chargers can be installed in location $j \in N$.

Some locations, namely those in $N' \subseteq N$, also represent population centers, each $i \in N'$ having r_i residents. It is possible that some of these residents already own EVs, as of the start of the first period in T; we refer to it as the initial demand of the corresponding center. In their daily routines, residents of location $i \in N'$ are willing to charge their vehicle in other neighboring locations, which we represent as $N_i \subset N$. A given share of each population center, $(1 - \gamma_i), i \in N', \gamma_i \in [0, 1]$, is assumed to have the capability to charge their vehicle at home and as such, its local charging demand does not need to be covered by the public infrastructure.

In this problem, charging stations are capacitated, and we thereby define a bound on how many drivers can be assigned to charge in each, at each time period, based on the number of chargers installed. This way of defining charger capacity follows previous approaches proposed for other capacitated siting problems (see, e.g., Upchurch et al., 2009; Zhang et al., 2017). These bounds a^t, $t \in T$, depend on (i) the anticipated best-case "active" period for a charging station (e.g., it is unrealistic to assume people are willing to charge at any time of the day), (ii) the average charge duration, (iii) the average driver mileage, and (iv) the average EV range.

As explained in the previous section, we assume that future EV adopters expect to be able to travel to other farther destinations. As such, we define a highway network $G = (N^R, A)$, where $N^R \subseteq N$ (it might be that $N^R \bigcap N' \neq \emptyset$) is the set of road nodes, and A represents the set of road segments, each connecting two nodes in N^R. Previous works on flow-based problems, such as the FLRP, have revealed that siting problems quickly become computationally intractable as the number of OD pairs grows; as such, rather than considering the routes between every pair of locations in N', we cluster them by larger urban zones, and ensure that EV drivers can travel between those. Let $N_u \subseteq N'$ be the set of population centers belonging to urban zone $u \in U$; we assume that every population center is assigned to one and only one urban zone. The geographical spread of the locations in each zone should be reasonably compact and within a limited radius, e.g., a given urban zone $u \in U$ might represent a mid-sized city, and each location in N_u, a neighborhood within that city. Note that it is possible to have $j \in N_i, j \in N_u, i \in N_v : u \in U, v \in U, u \neq v$, i.e., in their daily routines, residents of a given population center might be willing to charge in a location that does not belong to the same urban zone but to an adjacent one.

Let d_{uv} be the likelihood of EV drivers based in $u \in U$ traveling to $v \in U$, and $\alpha \in]0, 1[$ is a parameter estimating how often EV owners charge close to home, rather than on long-haul travels. In the instances presented in Section 6.2, we estimate the value of each d_{uv} following the gravity spatial interaction model Fotheringham and O'Kelly (1989) $\frac{r_u \cdot r_v}{\Delta_{uv}{}^2}$ where Δ_{uv} is the total length of the shortest path between u and v in G, and normalized such that $\sum_{v \in U} d_{uv} = 1, u \in U$. For the sake of simplicity, each urban zone is represented by a node in N^R, which can be seen as the access of the respective population centers to the highway network (as such, we designate it as access node). We define P_{uv} as the set of paths that drivers in u are willing to take to get to v; normally this will include the shortest, plus a few others whose length does not differ too much from that of the shortest. Some previous works have considered *all* so-called path deviation for each OD pair (see previous section). Even though the model proposed in the next section does not impose any restrictions on the number of these paths, in the computational experiments described in Section 6, we adopt a more conservative approach, and assume that mainstream customers are not too willing to compromise their daily habits when deciding whether or not to adopt EVs, and only consider a few possible path deviations.

Let N^p_{uv} and A^p_{uv} be, respectively, the set of nodes and the set of road segments on path $p \in P_{uv}$ sorted from origin to destination. Some road segments within A^p_{uv}, at the beginning of each path, can be reached without the need for recharging; we denote as A^{pt}_{uv} those that cannot, based on the average EV range at period $t \in T$. We denote as $N^{pt}_{uva} \subseteq N^p_{uv}$ the set of candidate nodes along the path between u and v, where drivers can (and must) charge their EV in order to reach the end node in road segment $a \in A^{pt}_{uv}$. These cover sets are easily computed, by investigating which nodes in N^p_{uv} are upstream of each road segment a and within the reach of EVs range. With this approach, we are able to handle paths of any length, even those that may require more than one recharging to be completed. Moreover, the only restriction imposed on the length of an arc in A is that it cannot exceed the length of the minimum average EV range. For details on how to calculate these sets we refer the reader to Capar et al. (2013) and Hosseini et al. (2017). Note that in these works, OD pairs are represented as bidirectional; hence, two sets of candidate nodes are created for each pair, one per direction. Here we instead represent each OD pair as unidirectional, as d_{uv} might be distinct from d_{vu}.

The goal of the proposed optimization problem is to maximize the number of EVs at the end of the last period in T. Let H^t_u be the number of EVs based in zone $u \in U$, at the beginning of period $t \in T$. The number of potential new EV owners in zone u at each period is given by a piecewise linear function of the number of EVs in the previous one, $\phi(H^{t-1}_u)$. The model imposes no conditions on the general shape of this function, other than it being continuous, non-decreasing and smaller than r_u, where $r_u = \sum_{i \in N_u} r_i$. The set of segments in the piecewise linear function associated with $u \in U$ is denoted as S_u. Each segment $s \in S_u$ is bounded by two breakpoints, q^{s-1}_u and q^s_u, and characterized by a slope m^s_u and an intercept o^s_u. Henceforth, we say that urban zone $u \in U$ is at penetration level $s \in S_u$ during period $t \in T$ if $q^{s-1}_u \leq h^{t-1}_u \leq q^s_u$. This notation is illustrated in Fig. 1. In the next section, we assume that at each period, the distribution of new drivers among the locations in N_u is proportional to the population of each of these centers. Nevertheless, the model also allows for any other type of distribution, should the data be available. Finally, we consider that out of these potential new EV owners, only those who have charging availability in their neighborhood and along the way to other urban zones, ultimately decide to purchase an EV.

Problem extensions. Finally, we identify a few possible extensions to this problem that can be of interest to decision makers this study. For the sake of compactness, we do not address

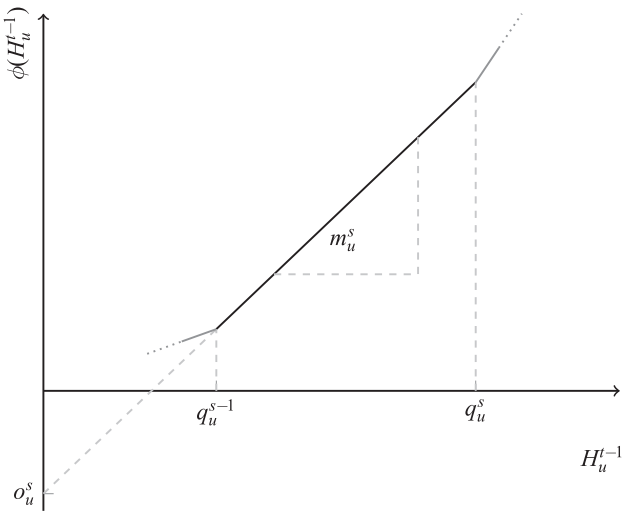

Fig. 1. Notation for each segment of $\phi(h_u^{t-1})$.

them in this paper. However, they can be tackled by our proposed model and solution method with only a few minor tweaks. First, we assume that only Level 3 or FastDC chargers will be installed (see Section 1), but our approach can be easily adapted to consider multiple types of charging stations. Second, we associate local charging with where people live, but the model is equally applicable to the case where local charging reflects where people work. The model can also be extended in such a way that local charging is both close to where people live and where people work. In this case, local demand should instead be associated with tuples of home and work location to ensure that no EV owner is counted twice.

4. Model

In this section, we present an MILP model for the problem described in the previous section. We first define the following sets of decision variables:

- x_j^t : number of chargers to be installed in location $j \in N$ at the beginning of period $t \in T$;
- y_j^t : 1 if a charging station is opened in $j \in N$ at the beginning of period $t \in T$, 0 otherwise ($y_j^1 = 1$ if $l_j > 0$);
- w_u^{st} : 1 if urban zone $u \in U$ is at penetration level $s \in S_u$ at the beginning of period $t \in T$, 0 otherwise;
- z_u^{st} : number of EVs based in urban zone $u \in U$ which is at penetration level $s \in S_u$ at the beginning of period $t \in T$;
- h_{ij}^t : number of EVs based in population center $i \in N'$ charging at a station in location $j \in N_i$ by the end of period $t \in T$;
- f_{uv}^{pt} : number of EVs traveling from $u \in U$ to $v \in U$ $(u \neq v)$ via path $p \in P_{uv}$ during period $t \in T$;
- g_{uvj}^{pt}: number of EVs traveling from $u \in U$ to $v \in U$ $(u \neq v)$ via path $p \in P_{uv}$ and charging at a station in location $j \in N_{uv}$, during period $t \in T$.

Note that $H_u^t := \sum_{i \in N_u} \sum_{j \in N_i} h_{ij}^t$. Using these variables, and the notation presented in the previous section and summarized in Table 1, we provide the formulation (1)–(21).

Constraint (2) limits the cost of the full investment. Constraints (3) additionally impose a budgetary limit on the investment made at each period. Constraints (4) and (5) bound the number of chargers that can be installed in each location. At the same time, together with inequalities (6), constraints (4) guarantee that the capital cost is paid when a charging station is opened at each location

Table 1
List of parameters.

T	set of investment periods
N	set of candidate locations
N'	set of population centers
U	set of urban zones
N_i	set of neighboring locations that residents of population center $i \in N'$ are willing to charge on a day-to-day
N_u	set of population centers belonging to urban zone $u \in U$
B	overall budget
b^t	budget of period $t \in T$
c^U	installation cost per charger
c_j^F	capital cost of opening a charging station in location $j \in N$
l_j	number of chargers already sited in location $j \in N$
e_j	maximum number of chargers that can be installed in location $j \in N$
r_i	population of center $i \in N'$
r_u	total population of urban zone $u \in U$
S_u	set of set segments in the growth function ϕ of urban center $u \in U$
q_u^{s-1}	lower breakpoint of segment $s \in S_u$
q_u^s	upper breakpoint of segment $s \in S_u$
m_u^s	slope of segment $s \in S_u$
o_u^s	intercept of segment $s \in S_u$
α	share of charges that the average EV owner does close to home, rather than on long-haul travels
γ_i	share of drivers in $i \in N'$ that do not have access to home charging
d_{uv}	likelihood of EV drivers based in $u \in U$ traveling to $v \in U$
P_{uv}	set of preferred paths from $u \in U$ to $v \in V$
N_{uv}^p	set of nodes in path $p \in P_{uv}$
A_{uv}^{pt}	set of arcs in path $p \in P_{uv}$, that EVs coming from u cannot reach during period $t \in T$, without charging the battery at an intermediary stop
N_{uva}^{pt}	set of candidate nodes along path $p \in P_{uv}$, where drivers can charge their EV in order to arrive at the end node of road segment $a \in A_{uv}^{pt}$
a^t	capacity of each charger, during period $t \in T$

(and not before nor after). In constraints (7), we calculate the number of EVs that exist in each urban zone at the beginning of each period; through the bounds (8), we ensure that this value is assigned to the z variable corresponding to the correct penetration level. Naturally, at any period, each location can only be at a single penetration level (9). Thereby, in the right hand side of (10), we determine the number of potential new EVs at every zone; as stated in the previous section, we assume that their distribution among the centers within the zone is proportional to their respective population.

The objective is to maximize the total number of EVs at the end of the last period (1). The number of EVs in each location at the end of each period is bounded by the number of potential new drivers (10), the number of EVs in the previous period (11), and the availability of charging opportunities (12)–(14). Constraints (12) determine the number of EVs that must travel between each pair of urban zones, through each of the paths connecting them. In constraints (13), we ensure that these paths can be completed given the EVs limited range; thus, those vehicles traveling on the path $p \in P_{uv}$ during period $t \in T$, must charge their vehicle in one of the nodes in N_{uva}^{pt}, if they are to arrive at arc $a \in A_{uv}^{pt}$. Finally, constraints (14) bound the number of EVs that can be assigned to charge at each location, given the number of chargers installed there.

Note that for $t = 1$, the right hand side of (7) should be replaced by the initial demand of the respective location. In (11), the left hand side should also be replaced by the share of initial demand for which the decision maker must guarantee coverage. It should be noted, though, that enforcing a high coverage guarantee can lead to instances for which there is no feasible solution due to the budgetary restrictions of the first period. For this reason, in the experiments described in Section 6, we impose no such lower bound. The impact of this omission on the long term decisions is expected to be minimal since the number of early EV adopters is still very small; moreover, as seen in Section 1, these EV owners

are likely to have charger access at home.

$$\max_{w,x,y,z\ f,g,h} \sum_{i\in N'} \sum_{j\in N_i} h_{ij}^{|T|} \tag{1}$$

$$\sum_{j\in N} \sum_{t\in T} (c^U x_j^t + c_j^F y_j^t) \le B \tag{2}$$

$$\sum_{j\in N} (c^U x_j^t + c_j^F y_j^t) \le b^t, \qquad t \in T \tag{3}$$

$$\sum_{t'\le t} x_j^{t'} + l_j \le e_j \sum_{t'\le t} y_j^{t'}, \qquad j \in N, t \in T \tag{4}$$

$$\sum_{t\in T} y_j^t \le 1, \qquad j \in N \tag{5}$$

$$y_j^t \le x_j^t, \qquad j \in N : l_j = 0, t \in T \tag{6}$$

$$\sum_{s\in S_u} z_u^{st} = \sum_{i\in N_u} \sum_{j\in N_i} h_{ij}^{t-1}, \qquad u \in U, t \in T \tag{7}$$

$$q_u^{s-1} w_u^{st} \le z_u^{st} \le q_u^s w_u^{st}, \qquad u \in U, s \in S_u, t \in T \tag{8}$$

$$\sum_{s\in S_u} w_u^{st} \le 1, \qquad u \in U, t \in T \tag{9}$$

$$\sum_{j\in N_i} h_{ij}^t \le \sum_{j\in N_i} h_{ij}^{t-1} + \frac{r_i}{r_u} \sum_{s\in S_u} \left(o_u^s w_u^{st} + (m_u^s - 1) z_u^{st}\right), \quad u \in U, i \in N_u, t \in T \tag{10}$$

$$\sum_{j\in N_i} h_{ij}^{t-1} \le \sum_{j\in N_i} h_{ij}^t, \qquad i \in N', t \in T \tag{11}$$

$$(1-\alpha)\, d_{uv} \sum_{i\in N_u} \sum_{j\in N_i} h_{ij}^t \le \sum_{p\in P_{uv}} f_{uv}^{pt}, \qquad u \in U, v \in U, t \in T \tag{12}$$

$$f_{uv}^{pt} \le \sum_{j\in N_{uva}^{pt}} g_{uvj}^{pt}, \qquad u \in U, v \in U, p \in P_{uv}, a \in A_{uv}^{pt}, t \in T \tag{13}$$

$$\alpha \sum_{i\in N_j} \gamma_i h_{ij}^t + \sum_{\{u,v\}\in U^2} \sum_{p\in P_{uv}} \sum_{j\in N_{uv}^p} g_{uvj}^{pt} \le a^t \,(l_j + \sum_{t'\le t} x_j^{t'}), \qquad j \in N, t \in T \tag{14}$$

$$x_j^t \in \mathbb{N}^0, \qquad j \in N, t \in T \tag{15}$$

$$y_j^t \in \mathbb{B}, \qquad j \in N, t \in T \tag{16}$$

$$w_u^{st} \in \mathbb{B}, \qquad u \in U, s \in S_u, t \in T \tag{17}$$

$$z_u^{st} \ge 0, \qquad u \in U, s \in S_u, t \in T \tag{18}$$

$$f_{uv}^{pt} \ge 0, \qquad u \in U, v \in U, p \in P_{uv}, t \in T \tag{19}$$

$$g_{uvj}^{pt} \ge 0, \qquad u \in U, v \in U, p \in P_{uv}, j \in N_{uv}^p, t \in T \tag{20}$$

$$h_{ij}^t \ge 0, \qquad i \in N', j \in N_i, t \in T \tag{21}$$

5. Rolling horizon heuristic

We solve the formulation proposed in the previous section using the state-of-the-art MILP solver CPLEX. However, as will be shown in Section 6, CPLEX often struggles to produce good primal solutions. As such, we present in this section a primal heuristic that is more efficient in creating good feasible solutions. This heuristic is the base of our proposed solution method, where we use it to warm start CPLEX.

In this heuristic, we solve our problem on a rolling horizon, i.e., we approach the problem iteratively, considering a single period at a time. In each iteration, the objective is to maximize the total number of EVs at the end of the corresponding period, while assuming that decisions undertaken in previous iterations are fixed. The proposed rolling horizon is a so-called forward-myopic method, as it solves periods in a chronological order. Similar heuristics have been used in the past to solve other multi-period problems (see, e.g., Chung & Kwon, 2015; Li et al., 2016; Zhang et al., 2017). In addition to a forward-myopic rolling horizon, a backward-myopic method is also proposed in Chung and Kwon (2015). Note that such a method cannot be devised for problems with dynamic demand like ours, where the demand to be covered in one period depends on the siting decisions made in previous ones.

Formulation (22)–(36) represents the sub-problem that must be solved at each iteration, for period $\bar{t}$; we represent siting decisions that are fixed by $\bar{x}$ and $\bar{y}$, whereas x and y continue to be decision variables. Even though we must solve $|T|$ MILP subproblems, each subproblem is much easier than the complete multi-period one, mainly because the number of potential new EV adopters becomes exogenous to the optimization problem. As such, it is not necessary to use the many variables and constraints necessary to model the piecewise linear growth function, as in the original multi-period formulation. In constraints (28), we represent the lower and upper bounds on the number of EVs by $\bar{h}^-$ and $\bar{h}^+$, respectively; for each $i \in N'$, $\bar{h}_i^- := \sum_{j\in N_i} h_{ij}^{\bar{t}-1}$ and $\bar{h}_i^+ := \bar{h}_i^- + \frac{r_i}{r_u}\left(o_u^{\bar{s}_u} + (m_u^{\bar{s}_u} - 1) H_u^{\bar{t}-1}\right)$, where $u \in U$ is such that $i \in N_u$ and $\bar{s}_u : q_u^{\bar{s}_u - 1} \le H_u^{\bar{t}-1} \le q_u^{\bar{s}_u}$.

This heuristic is greedy with respect to the available budget resources. This means that this procedure always prioritizes investment in the incumbent period (as long as it maximizes the number of EVs at the end of it), even if that expenditure may be more consequential in subsequent periods. As a result of that, the relative quality of the solution created by this heuristic might worsen when $\Sigma_{t\in T} b^t \gg B$. We analyze this in our computational experiments, whose results are presented in Section 6.

It might happen that at a given period all the existing and potential new EV drivers at every location can be served, without the need to spend all the installation budget available for that period. Nevertheless, it does not make sense to leave these funds unused. Indeed, at a later period, the possibility of having a higher EV adoption might be conditional to the existence of more chargers than those already sited plus those that can be newly installed given the respective period-specific budget. Therefore, at each iteration, we allow for new siting decisions to be made retroactively, and assigned to the budget of a past period (as long as it has not been already complete allocated, naturally). For this reason, at each iteration of our rolling horizon, our formulation features variables x (32) and y (33) associated with the incumbent period, as well as with all the preceding periods; nevertheless, the value of those corresponding to decisions already defined in previous iterations are fixed, and cannot be changed.

In the next section, we discuss some further details on the implementation of this heuristic.

$$\max_{\substack{x,y\\f,g,h}} \sum_{i\in N'} \sum_{j\in N_i} h_{ij} \tag{22}$$

$$\sum_{j\in N} \sum_{t\le \bar{t}} (c^U x_j^t + c_j^F y_j^t) \le B - \sum_{j\in N} \sum_{t<\bar{t}} (c^U \bar{x}_j^t + c_j^F \bar{y}_j^t) \tag{23}$$

$$\sum_{j\in N} (c^U x_j^t + c_j^F y_j^t) \le b^t - \sum_{j\in N} (c^U \bar{x}_j^t + c_j^F \bar{y}_j^t), \qquad t \le \bar{t} \tag{24}$$

$$\sum_{t'\le t} (x_j^{t'} + \bar{x}_j^{t'}) + l_j \le e_j \sum_{t'\le t} (y_j^{t'} + \bar{y}_j^{t'}) \qquad j \in N, t \le \bar{t} \tag{25}$$

$$\sum_{t\le \bar{t}} y_j^t \le 1, \qquad j \in N : \sum_{t'\le t} \bar{y}_j^{t'} = 0 \tag{26}$$

$$y_j^t \le x_j^t, \qquad j \in N : l_j = 0 \wedge \sum_{t'\le t} \bar{y}_j^{t'} = 0, t \le \bar{t} \tag{27}$$

$$\bar{h}_i^- \le \sum_{j\in N_i} h_{ij} \le \bar{h}_i^+, \qquad i \in N', t \in T \tag{28}$$

$$(1-\alpha) d_{uv} \sum_{i\in N_u} \sum_{j\in N_i} h_{ij} \le \sum_{p\in P_{uv}} f_{uv}^p, \qquad u \in U, v \in U, \tag{29}$$

$$f_{uv}^p \le \sum_{j\in N_{uva}^{p,\bar{t}}} g_{uvj}^p, \qquad u \in U, v \in U, p \in P_{uv}, a \in A_{uv}^{\bar{t}} \tag{30}$$

$$\alpha \sum_{i\in N_j} \gamma_i h_{ij} + \sum_{\{u,v\}\in U^2} \sum_{p\in P_{uv}} \sum_{j\in N_{uv}^p} g_{uvj}^p \le a^{\bar{t}} \left(l_j + \sum_{t\le \bar{t}} (x_j^t + \bar{x}_j^t)\right), \qquad j \in N \tag{31}$$

$$x_j^t \in \mathbb{N}^0, \qquad j \in N, t \le \bar{t} \tag{32}$$

$$y_j^t \in \mathbb{B}, \qquad j \in N : \sum_{t'\le t} \bar{y}_j^{t'} = 0, t \le \bar{t} \tag{33}$$

$$f_{uv}^p \ge 0, \qquad u \in U, v \in U, p \in P_{uv} \tag{34}$$

$$g_{uvj}^p \ge 0, \qquad u \in U, v \in U, p \in P_{uv}, j \in N_{uv}^p \tag{35}$$

$$h_{ij} \ge 0, \qquad i \in N', j \in N_i \tag{36}$$

6. Computational experiments

In this section, we (i) provide more details on the implementation of our proposed solution methods (Section 6.1), (ii) present a test set with instances based on multi-scale siting landscapes (Section 6.2), and (iii) analyze the results of computational experiments performed using the test set to assess and compare the capabilities of the proposed methods.

Note that every network, growth function and set of parameters described in Section 6.2 was created for the sole purpose of testing the computational efficiency of the proposed solution methods, and we make no claims regarding its realism. However, we emphasize that our model is flexible enough that more precise and representational data can be used if available.

6.1. Implementation

We implement the formulation (1)–(21) in `IBM ILOG CPLEX 12.8` using its `Java API`, and solve each instance of the problem using `CPLEX` standard solving method. Based on our preliminary experiments, we set `CPLEX` parameters such that it uses the `Barrier` method as the linear programming (LP) solver at the root node, and the `Dual` method in all others. Before running the solver, we determine which variables w and z can be fixed to zero *a priori*, by computing in the pre-processing phase the highest penetration level each urban zone can be at, in a hypothetical best-case scenario where local and inter-city charging availability is maximal (given bounds e_j, $j \in N$ - see Section 3). For the sake of simplicity, in Section 6.3, we denote this approach as `CPLEX` in the tables and graphs presenting the results of computational experiments.

Our proposed solution method `SM` extends the latter by first running the primal heuristic presented in Section 5, and using the feasible solution generated by it to warm start `CPLEX` (via the `MILP start` functionality). At each iteration of the primal heuristic, we solve formulation (22)–(36), by using the same LP solver configuration as above, and by setting `CPLEX MILP emphasis switch` parameter settings to prioritize the search for feasible solutions over the proof of optimality. We impose a time limit for this heuristic of half the length of the time limit established for the entire `SM`. In preliminary experiments, we observed that the MILPs at the first iterations tend to be more challenging for `CPLEX` than the ones at later iterations. As such, we do not divide the aforementioned time limit equally, but instead allow the first $\lfloor \frac{|T|}{2} \rfloor$ iterations to run for a longer time than the others. If an iteration is completed before its respective time limit, the remaining time is added to the time limit of the subsequent iteration; an iteration is completed if a feasible solution to the corresponding MILP is found, and is proven to have a relative optimality gap of at most 1%.

All experiments are run on a single core within the Graham cluster of Compute Canada (Intel “Broadwell” CPUs at 2.1. GHz).

6.2. Test set

To test the computational performance of our solution methods, we created two networks, that represent siting locations in the province of Quebec in Canada, and in the state of California in the U.S.. Both regions have large geographical areas, and governments committed to the goal of electrifying their road transportation. (These instances are openly accessible in Anjos et al., 2019).

Quebec network. We denote as `Quebec`, the network depicted in Fig. 2. This network has 2363 candidate locations, out of which 547 are population centers represented by gray nodes. Each center has an average population of 11,580, with the numbers of residents ranging from 7111 to 20138. The location and population of these centers is based on data of the Canadian 2016 census Canada (2018). However, they do not have a one-to-one correspondence to real census subdivisions, but rather represent aggregations of “reasonably” populous municipalities; thereby, the sum of all residents considered in this instance represents 78% of the total population of the Quebec province. We aggregated these locations in 40 urban zones, whose access nodes are represented in Fig. 2 by a star shape; they were selected such that every population center was within 30 kilometer of its assigned access node. Each population center was also given an initial demand, randomly generated from a Normal distribution with mean of 0.2% of each center’s population.

Finally, the 1816 white circles in Fig. 2 represent candidate locations along the main roads in Quebec’s highway system. The distance between two sequential road nodes fluctuates slightly, but

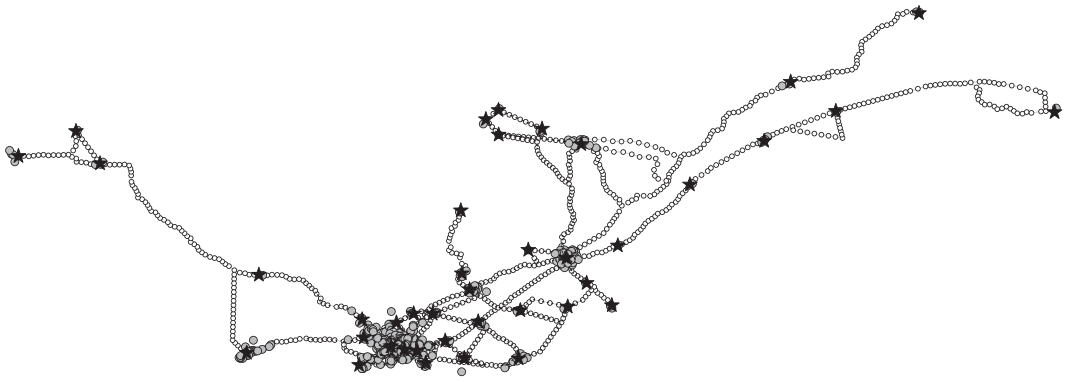

Fig. 2. Quebec network.

Table 2
Topological characteristics of the Quebec subnetworks.

n_zones	n_centers	max_width	road_precision
5	20	200	5
10	50	600	10
20	100	1000	15
30	300	∞	

is never less than 10 kilometer; we define this distance as the road_precision. For each pair of urban zones, whose minimum road distance is greater than half of the average EV range (see "Remaining parameters"), we computed up to five paths that EV drivers are willing to take to travel between them. To generate these paths, we calculated the five shortest paths, but imposed additional conditions ensuring that (i) none can exceed the distance of the shortest path by more than 10%, and (ii) they must differ from the others in at least 10% of their length.

We assigned already-existing fast charging stations to nearby locations, following data from Quebec's *Circuit électrique* Cir (2018); there were 71 fast chargers when this network was created.

Quebec subnetworks. To better understand how different topological characteristics of the siting landscape might impact the performance of the proposed solving methods, we also randomly generated 150 additional network-instances, each a subnetwork of the Quebec network described above. In addition to the aforementioned road_precision, we define the following parameters: n_zones ($|U|$), n_centers ($|N'|$), and max_width (the maximum road distance observed among all of the shortest paths connecting two urban zones selected in the subnetwork). Table 2 details, for each of these parameters, all the values that were used to generate the different subnetworks. An instance was created for every possible combination of these values, with the following exceptions for which no subnetworks of Quebec exist: (i) n_zones $= \{20, 30\}$ and n_centers $= 20$, and (ii) n_zones $= \{20, 30\}$ and max_width $= 200$.

California network. We designate by California, our second large-size network depicted in Fig. 3. This instance has 4608 candidate locations, including 1832 population centers. The population of each center ranges from 5006 to 137,779 residents, with the average being of 14901. We used data from the 2010 U.S. census (Bureau, 2018) to generate these centers, but simplifications were made as was the done for the Quebec instance (see "Quebec network"); as such, the population included in our instance-network corresponds to 73% of the total population of the state of California as of 2010. These population centers were clustered in 75 urban zones, which were selected such that every center is within 15 kilometer of their respective access node. Each population center was assigned a randomly-generated initial demand (Normal distribution with mean of 0.95% of the center's population). The remaining 2776 nodes represent candidate locations along the roads of California's highway network, with a road_precision of 10 kilometer. Following the same rules described above for the Quebec case, we generated up to 5 possible routing paths between every pair of urban zones. We assigned 1408 of the fast chargers that existed as of the creation of this network to nearby locations (data from the U.S. Department of Energy States, 2018).

Growth function ϕ. In Fig. 4, we represent how EV adoption has grown from 2010 to 2017 in Belgium, France, California, Norway, Sweden and the UK, based on publicly-available data on new EV registrations from the European Alternative Fuels Observatory (EAF, 2018) and the California New Car Dealers Association (Association, 2018). This data is typically displayed as the total number of EVs per year. We plot it in Fig. 4 in a different way, following the structure of our growth function, and show the number of EVs in a given year, given how many EVs were registered in the previous year. We observe in Fig. 4 that this growth is quasi-linear, with a slight concavity. Nevertheless, it is hard to predict how these curves will behave in the future because as current EV adoption levels are still quite distant from those in some governmental targets. For example, it is possible that in some countries the curves will become convex in coming years. Regardless, one thing is certain: at some point the slope of these curves will tend to zero, as fewer and fewer potential new EV drivers remain, and markets become saturated.

In our experiments, we assume that each period represents one year, and we use the growth function in Fig. 5. This function extends the trend of the California EV adoption growth until 25% of the population owns an EV; at that point, we assume there is an inflection and the growth rate reduces thus simulating the aforementioned plateauing effect. Finally we assume a limit of $\sim$42% EV adoption, representing market saturation. The resulting function has four segments, with breakpoints 0, 0.0007, 0.25, 0.4 and 0.42; and slopes 2.28, 1.23, 0.7 and 0.1 respectively. Intercepts can be calculated using the formula $o^s := o^{s-1} + (m^{s-1} - m^s)\, q^{s-1}$, with $o^0 = 0.0002$.

Remaining parameters. At each population center we limit the number of chargers to be installed in each station at 16; in all other locations, we only allow up to 8 chargers to be installed, i.e., $e_j = 16,\ j \in N'$ and $e_j = 8,\ j \in N \backslash N'$. Moreover, we impose an installation cost per chargers of \$22.5k (c^U), and a one-time cost of opening a station of \$45k for road nodes ($c^F_j,\ j \in N \backslash N'$) (Zhang et al., 2017) and of \$60k for population centers ($c^F_j,\ j \in N'$); in Zhang et al. (2017), only one type of location is considered, but here we assume that the land purchase cost is higher in population centers. We consider a \$100M total budget for the instance using the full Quebec network, and 10 investment periods. Since

Fig. 3. `California` network.

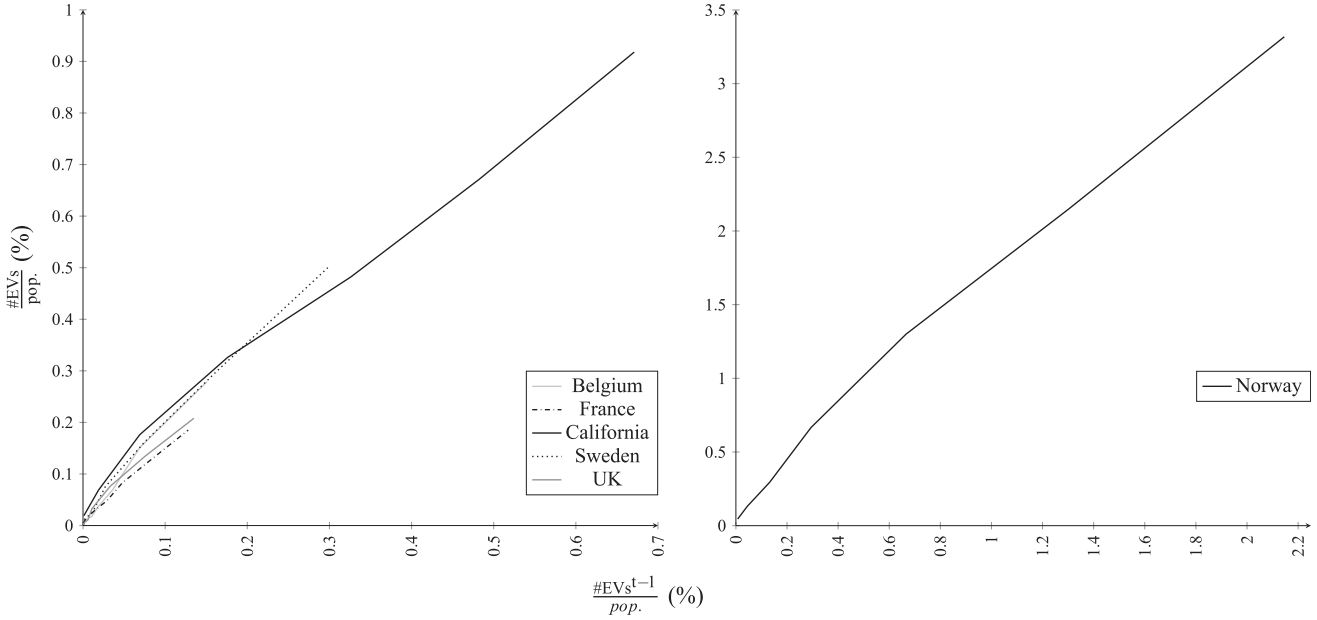

Fig. 4. EV adoption growth in Belgium, France, California, Norway, Sweden and UK from 2010 to 2017. This graph plots the share of the population that owns an EV in a given year, based on the share of the population that owned an EV in the previous year.

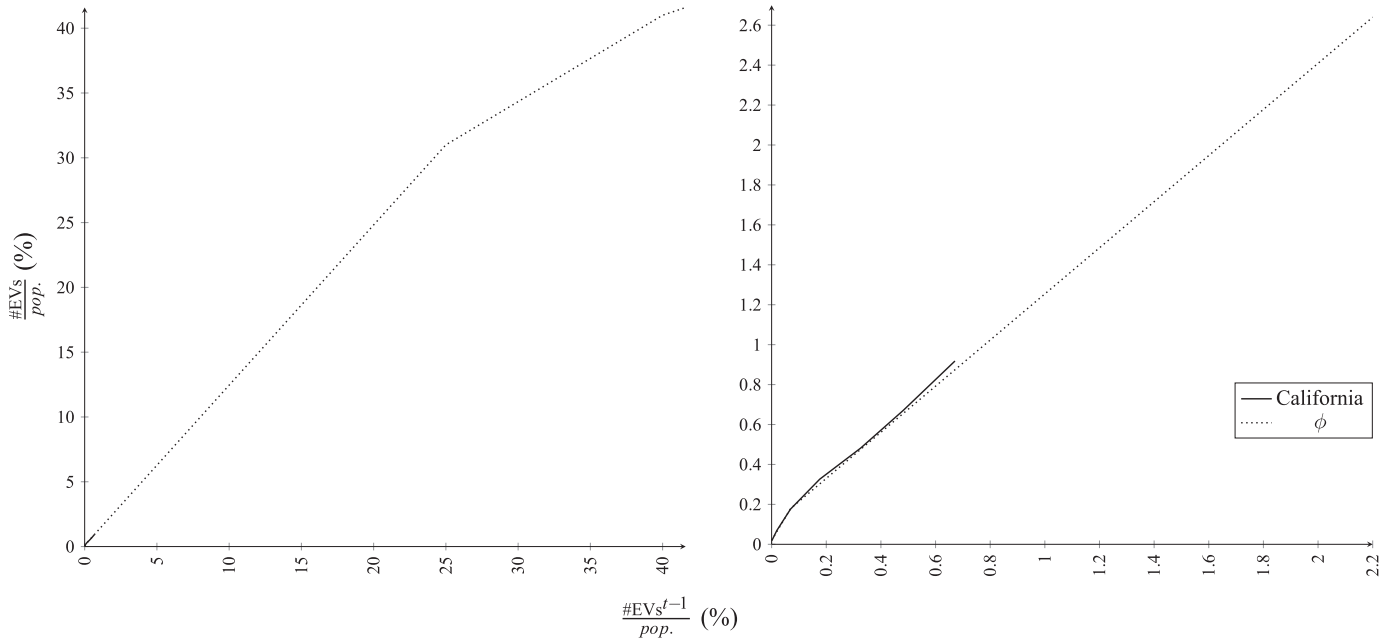

Fig. 5. Growth function ϕ used in computational experiments compared with California's real growth up until 2017. Functions presented in two different scales.

in our experiments we test subnetwork instances with different numbers of investment periods and total population, we set for every instance a budget of \$1.579 per resident and per period. We assume that the period-specific budget b^t, $t \in T$, is the same for every period; nevertheless, we allow for some flexibility in how the total funds can be allocated, i.e., $\Sigma_{t\in T} b^t > B$. Thus, we define $b^t = \frac{B}{|T|} \cdot (1+\beta)$, where β is a parameter regulating the aforementioned flexibility. We test scenarios with $\beta = 0.05$ (little flexibility), $\beta = 1$ (some flexibility), and $\beta = |T| - 1$ (full flexibility, i.e., there are no period-specific budgets, and only the overall budget limits the investment).

We consider that the average EV range is of 250 kilometer in the first period, with an increase rate of 1.1 per year. Nevertheless, we also expect that EV drivers typically prefer not to go below 20% of the capacity of the EV battery, due to range anxiety, so we assume that this range is of only 200 kilometer. As it was explained in Section 3, the average EV range has an impact on the charging needs of drivers on long travels, as well as on how many EVs each charger can serve, i.e., its capacity a. We estimate that each EV owner drives an average of 400 kilometer per week, which means two charges per week. We predict that in the best case scenario, charging stations will be used for only six hours per day, and each charge lasts 20 to 30 minutes. Based on these estimates, we define that the capacity of each charger is of 45 EVs in the first year (a^0), and it grows at a 1.1 rate per year ($a^t = 1.1\, a^{t-1}, t > 0$). For each population center $i \in N'$, we assume the set of neighboring locations N_i to be composed by every location within 10 kilometer of i. Furthermore, we set $\gamma_i = 0.8, i \in N'$, i.e., one in five EV drivers has access to home charging.

Finally, we test various scenarios with different time horizons, namely $|T| = 5$, $|T| = 10$ and $|T| = 15$, as well as different α values (see Section 3), $\alpha = 0.9$, $\alpha = 0.7$ and $\alpha = 0.5$.

6.3. Results

In this section, we present and analyze the results of computational experiments, in which we used CPLEX standard solving method and SM to solve the instances presented in Section 6.2. We first discuss how each solution method performs on Quebec subnetworks with different sizes, time horizons, and parameters α and β. In these experiments, we set a time limit of 7200 minutes and a memory limit of 16 Gigabyte. Then, we report the results of experiments with more demanding instances using the full Quebec and California network; for these tests we increase both the time limit and the memory limit twofold to 14,400 minutes and 32 Gigabyte respectively.

Quebec subnetworks. In Figs. 6 and 7, we depict performance profile graphs for the optimality gap, calculated as $\frac{ub-lb}{ub}$, where *ub* and *lb* are respectively the last primal and dual bounds produced by CPLEX at the end of time limit. In each figure, we present results for both CPLEX with (SM) and without the rolling horizon heuristic, and different planning horizons, $|T| = 5$, $|T| = 10$ and $|T| = 15$. In Fig. 6, we show these results for $\beta = 0.05$, and $\alpha = 0.9$, $\alpha = 0.7$ and $\alpha = 0.5$. In Fig. 7, we show them for $\alpha = 0.9$, and $\beta = 0.05$, $\beta = 1$ and $\beta = |T| - 1$. In Table 3, we show the minimum (*min*), average (*avg*) and maximum (*max*) value of different performance indicators, aggregated by instances with the same value for $|T|$, α and β. In the last row, all the results, with every parameter configuration, are aggregated. In addition to the aforementioned optimality gap (*opt. gap*), we present the following performance indicators: *runtime*, the number of instances for which no feasible solution is found by each method (*nLB*) and the number of instances for which SM is unable to find a dual bound (*nUB*) before the time and/or memory limits are exceeded, the runtime of the heuristic in SM (*runtime heur.*) and the relative gap between the objective value of the solution it produces and the final dual bound (*gap heur.*), and the EV adoption (as a proportion of the instance's total population) at the end of the last period, in the best solution found by SM (*adoption*).

We first observe that no solution method performs clearly better than the other with respect to finding optimal solutions within the time limit of two hours. However, Figs. 6 and 7 show that the optimality gaps obtained with SM are clearly smaller than those obtained when not using the rolling horizon heuristic. This suggests that CPLEX struggles to produce good feasible solutions for the more demanding instances, and thus using the proposed heuristic beforehand is imperative. This is highlighted in Table 3, where we see that for 518 of all 2250 instances (23%), CPLEX cannot even find a single feasible solution without the rolling horizon heuristic. This is particularly striking given that we impose no

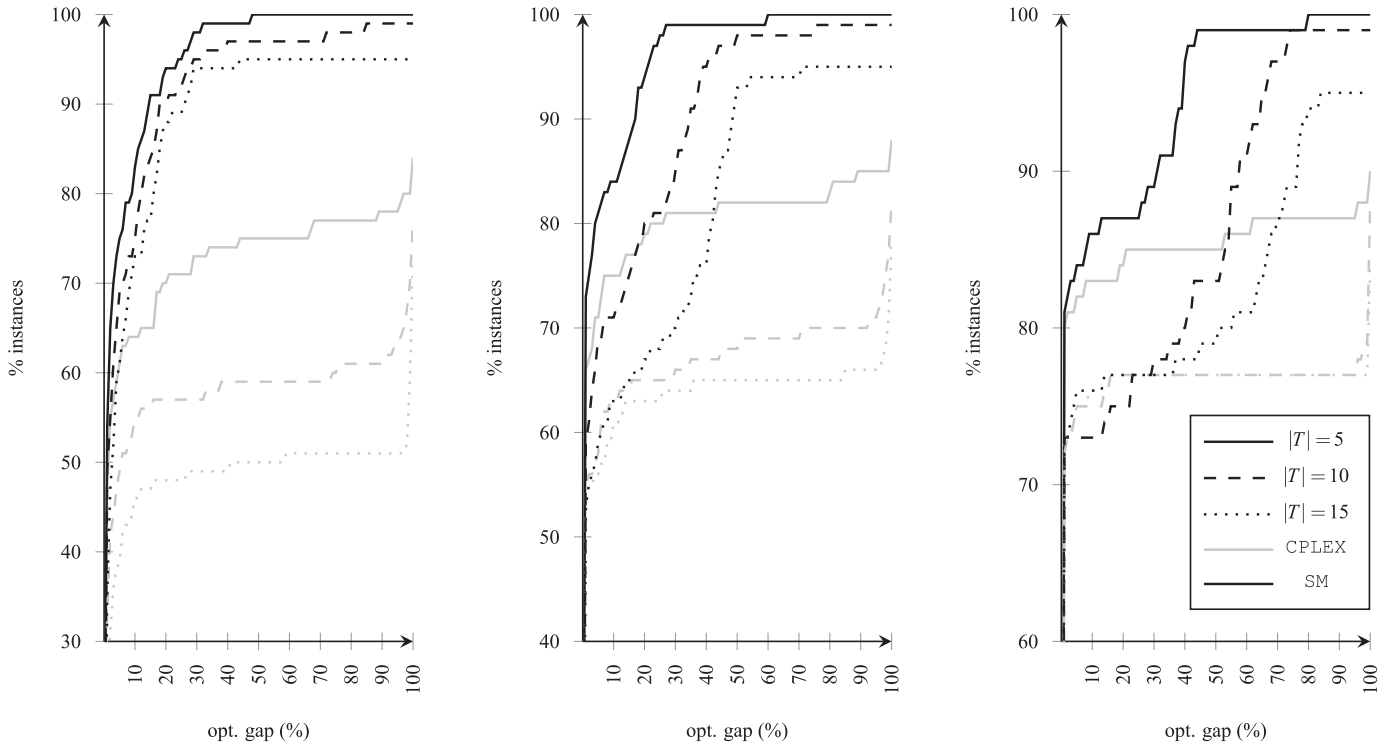

Fig. 6. Performance profile for optimality gaps (%) for all 150 instances based on the `Quebec` subnetworks, and for different values of the β parameter ($\alpha = 0.9$).

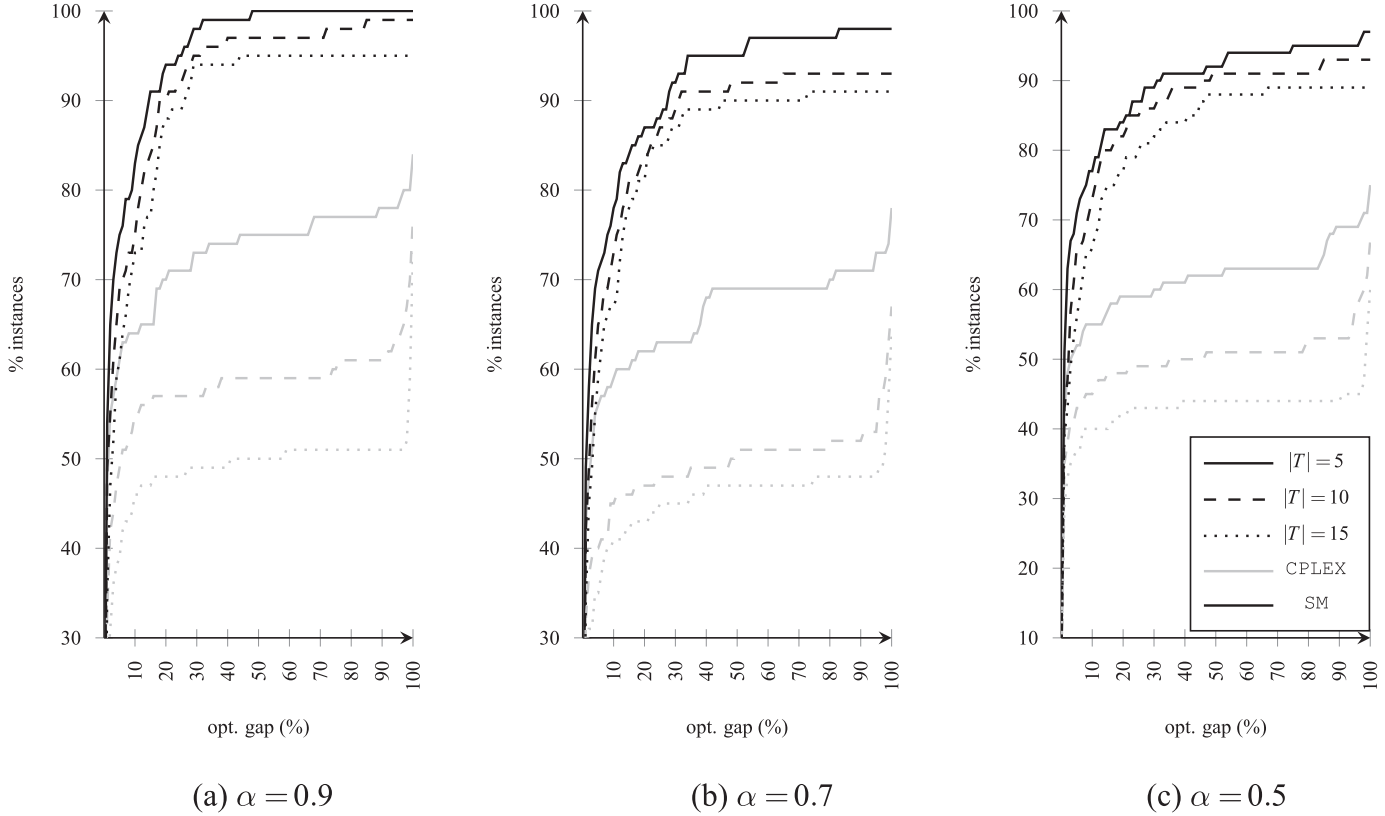

Fig. 7. Performance profile for optimality gaps (%) for all 150 instances based on the `Quebec` subnetworks, and for different values of the α parameter ($\beta = 0.05$).

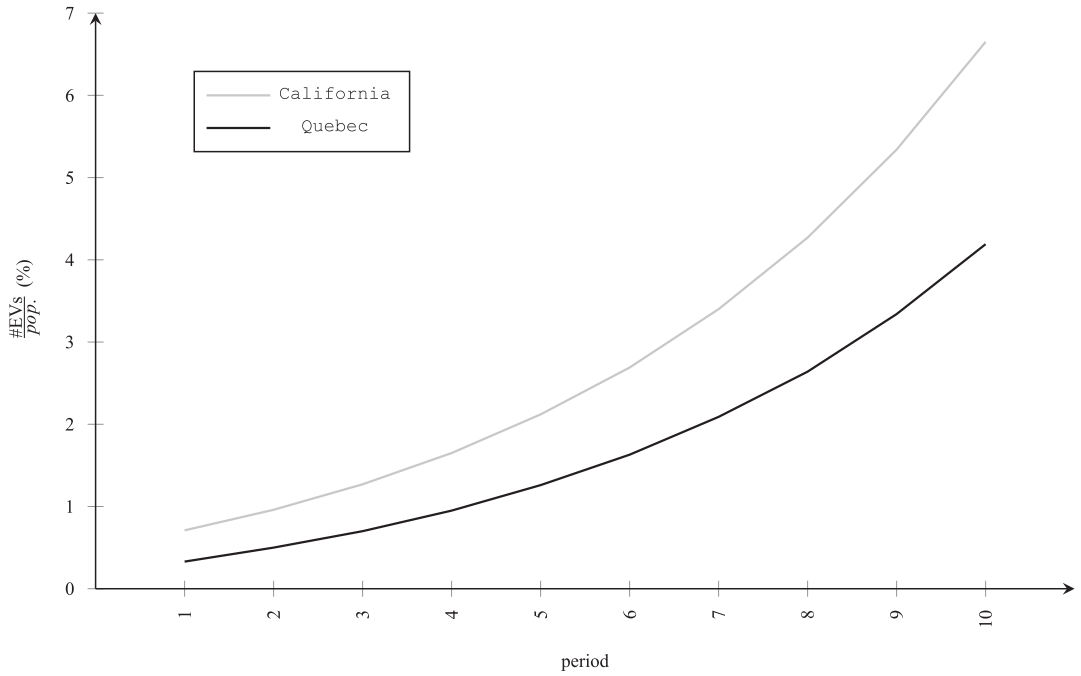

Fig. 8. Evolution of EV adoption over time, for the solution created by SM for the instances using both Quebec and California networks and $|T| = 10$.

lower bound in constraints (11), which means a solution where no charger is installed is a feasible one (see end of Section 4). By using SM, a feasible solution is found for 2160 instances (96%); for most of the remaining 90 instances, the heuristic is unable to produce a feasible solution due to out-of-memory issues. Moreover, the heuristic is quite efficient, and on average takes 400 seconds to produce a feasible solution (out of an imposed time limit of one hour). Finally, we note that the difference of quality between the solution produced by the proposed heuristic and the final solution found by SM, represented by *gap heur.* in Table 3, can be substantial, with an average value of 16%. This suggests that the heuristic should be seen as an important and helpful complement of the complete MILP formulation, but not as an alternative to it, since CPLEX is often able to improve the solution.

These results also allow us to understand how parameters $|T|$, α and β impact the difficulty of our problem and the performance of our solution methods. Unsurprisingly, the difficulty of the problem increases with the number of investment periods. The flexibility in budget-to-period allocation (represented by the β parameter) has a major influence on the percentage of instances that our solution methods solve to optimality within the time limit. For example, when $\beta = 1$ ($\beta = |T| - 1$), we are 2 (2.6) times as likely to achieve optimality within the time limit as when $\beta = 0.05$. It is easy to fathom why: by increasing the value of β, we are essentially "relaxing" constraints (3), therefore making the model easier to solve. Moreover, as the value of β grows, the positive effect of the heuristic fades and the performance of both methods becomes more and more similar, as explained in Section 5. We note that even though the number of instances solved to optimality for $\beta = 0.05$ is quite low, the quality of the final solutions produced by SM is high, as evidenced by the small optimality gaps in Fig. 6a. Finally, we see that the performance of SM is relatively consistent for different values of α, whereas the performance of CPLEX without the rolling horizon heuristic appears to worsen as α decreases.

In Table 4, we aggregate results by instances whose associated network share some topological characteristics, to help understand how the latter influence the performance of both methods. We see that the problem becomes harder when the values of `max_width` increase, and when the values of `road_precision` decrease; this is to be expected, since both trends are associated with a growing number of road nodes. Perhaps more surprising, though, is the observation that by increasing the number of population centers the problem becomes apparently easier. One reason for this may be that the size of formulations (1)–(21) and (22)–(36) (in particular the number variables h) does not grow too much based on the number of population centers directly, but rather as a function of the number of "neighbor" nodes. Yet, we also see that the problem tends to become more difficult as the overall spatial spread (defined by characteristics `n_zones` and `max_width`) between populations increases. This suggests that the main challenge of the proposed optimization problem lies in the road charging decisions, rather than in those related to the daily local charging. This reinforces the idea, introduced in Section 2, that solving siting optimization problems that model every type of charging demand as flow-based is impractical for large geographical landscapes.

Quebec and California networks. In Table 5, we show the results of computational experiments done over instances using the full Quebec and California networks, and different time horizons (we fix $\alpha = 0.9$ and $\beta = 0.05$). As was mentioned in the description of these networks in Section 6.2, we set a `road_precision` of 10 kilometer; as can be seen in Table 4, when `road_precision` $= 5$ kilometer, SM is much more likely to struggle in finding feasible solutions or to have out-of-memory issues. In the 4h time limit, CPLEX is only able to produce by itself a feasible solution for the instance with the Quebec network and with $|T| = 5$. Conversely, by using SM, we are able to find a feasible solution for every one of these large-size instances, with demonstrably good quality. For instances based on the Quebec network the optimality gaps never exceed 3%. For instances based on the California network, the gaps are slightly larger, 3.3%, 2.9% and 6.4% for 5, 10 and 15 periods respectively. Contrary to what happened in the previous set of experiments, CPLEX is unable to improve the solution generated by the heuristic for these larger instances. Regardless, we recommend to at least try to solve the root node of the full model, as the heuristic cannot provide a

Table 3
Summary of results for the experiments over all instances based on the `Quebec` subnetworks, aggregated by parameters $|T|$, α and β. The last row presents results for all instances and all values of these parameters.

			CPLEX							SM															
			nLB	runtime (s)			opt. gap (%)			nUB	nLB	runtime			opt. gap (%)			runtime heur. (s)			gap heur. (%)			adoption (%)		
		#	(#)	min	avg	max	min	avg	max	(#)	(#)	min	avg	max	min	avg	max	min	avg	max	min	avg	max	min	avg	max
$\|T\|$	5	750	128	0	4012	7200	0	12	100	8	1	1	3915	7200	0	6	98	0	438	5155	0	12	98	0.0	1.2	1.3
	10	750	178	1	4697	7200	0	21	100	27	3	1	4608	7200	0	8	88	0	422	5221	0	17	88	0.5	3.9	4.3
	15	750	212	1	4964	7200	0	23	100	55	0	2	4960	7200	0	9	84	1	337	3530	0	20	85	2.1	11.5	12.8
α	0.9	1350	234	0	3974	7200	0	15	100	30	0	1	3931	7200	0	8	84	0	282	4311	0	21	85	0.3	5.4	12.8
	0.7	450	137	2	5591	7200	0	23	100	27	3	1	5510	7200	0	7	88	0	554	4843	0	8	88	0.2	5.5	12.8
	0.5	450	147	3	5296	7200	0	24	100	33	1	3	5181	7200	0	8	98	0	615	5221	0	9	98	0.0	5.4	12.8
β	0.05	1350	383	2	5618	7200	0	23	100	70	4	1	5527	7200	0	7	98	0	532	5221	0	8	98	0.0	5.5	12.8
	1	450	78	1	3770	7200	0	15	100	10	0	1	3650	7200	0	8	76	0	248	4037	0	20	76	0.5	5.3	12.8
	$\|T\|-1$	450	57	0	2203	7200	0	9	100	10	0	1	2271	7200	0	10	84	0	166	4311	0	35	85	0.3	5.3	12.8
		2250	518	0	4548	7200	0	18	100	90	4	1	4483	7200	0	8	98	0	400	5221	0	16	98	0.0	5.4	12.8

Table 4
Summary of results for the experiments over all instances based on the `Quebec` subnetworks, aggregated by network topological characteristics `n_zones`, `n_centers`, `max_width` and `road_precision`.

			CPLEX							SM															
			nLB	runtime (s)			opt. gap (%)			nUB	nLB	runtime			opt. gap (%)			runtime heur. (s)			gap heur. (%)			adoption (%)		
		#	(#)	min	avg	max	min	avg	max	(#)	(#)	min	avg	max	min	avg	max	min	avg	max	min	avg	max	min	avg	max
`n_zones`	5	720	36	0	2878	7200	0	7	100	0	0	1	2715	7200	0	2	78	0	105	1753	0	10	80	0.7	5.9	12.8
	10	720	113	1	4561	7200	0	18	100	11	1	2	4497	7200	0	7	88	0	361	4278	0	16	88	0.5	5.4	12.8
	20	405	161	8	5964	7200	0	33	100	35	3	23	5956	7200	0	10	84	5	579	5155	1	19	84	0.6	5.1	12.8
	30	405	208	31	6387	7200	0	40	100	44	0	44	6461	7200	0	17	98	7	882	5221	1	26	98	0.0	4.7	12.8
`n_centers`	20	360	55	0	4347	7200	0	24	100	2	0	1	4089	7200	0	12	88	0	452	4278	0	24	88	0.5	5.1	12.8
	50	630	187	1	4886	7200	0	21	100	38	2	1	4854	7200	0	10	98	0	509	5221	0	20	98	0.0	5.2	12.8
	100	630	152	3	4489	7200	0	20	100	31	1	3	4461	7200	0	7	97	1	415	5155	0	15	97	0.0	5.5	12.8
	300	630	124	12	4394	7200	0	11	100	19	1	19	4376	7200	0	3	83	3	250	4843	0	8	83	0.2	5.8	12.8
`max_w.`	200	360	0	0	1343	7200	0	0	3	0	0	1	1348	7200	0	0	4	0	46	866	0	6	69	1.1	6.1	12.8
	600	630	44	2	3839	7200	0	11	100	0	0	3	3746	7200	0	2	44	1	206	2640	0	14	77	1.0	5.9	12.8
	1000	630	198	4	5744	7200	0	29	100	19	1	7	5694	7200	0	10	97	3	459	4514	0	19	97	0.0	5.2	12.8
	∞	630	276	8	6091	7200	0	35	100	71	3	10	6000	7200	0	16	98	5	780	5221	0	22	98	0.0	4.7	12.8
`road_p.`	5	750	300	1	5073	7200	0	18	100	86	4	2	4996	7200	0	11	97	1	642	5155	0	18	97	0.0	5.1	12.8
	10	750	165	1	4652	7200	0	20	100	4	0	1	4606	7200	0	9	98	0	383	5221	0	17	98	0.0	5.4	12.8
	15	750	53	0	3976	7200	0	16	100	0	0	1	3904	7200	0	4	76	0	202	1709	0	14	85	0.5	5.7	12.8

Table 5
Summary of results for the experiments using CPLEX and SM, over instances based on Quebec and California full networks, with $\alpha = 0.9$ and $\beta = 0.05$.

		CPLEX		SM				
network	$\|T\|$	runtime (s)	opt. gap (%)	runtime (s)	opt. gap (%)	runtime heur. (s)	gap heur. (%)	adoption (%)
Quebec	5	14,400	97	14,400	2.1	522	2.1	1.2
	10	14,400	∞	14,400	2.4	780	2.4	4.2
	15	14,400	∞	14,400	2.8	921	2.8	12.5
Calif.	5	14,400	∞	14,400	3.3	2256	3.3	2.1
	10	14,400	∞	14,400	2.9	5578	2.9	6.6
	15	14,400	∞	14,400	6.4	5431	6.4	18.9

Table 6
Evolution of charging infrastructure over time, for the solution created by SM for the instances using both Quebec and California networks and $|T| = 10$. The first set of rows indicate the total number of chargers (*# rows*) installed in population centers (*pop.*) and in the road network (*road*). The second set of rows indicate the number of nodes that have at least one charging station (*# nodes w/ station(s)*). The last set of rows indicate the percentage of road nodes that have at least one charger serving local charging demand (*% road nodes dual purpose*).

			period									
			1	2	3	4	5	6	7	8	9	10
# chargers	Calif.	pop.	796	2146	2755	3331	3684	4253	4789	5518	6107	6722
		road	612	1235	1799	2793	3974	5053	6179	6899	7988	8995
	Quebec	pop.	33	232	373	468	584	696	866	987	1126	1267
		road	38	180	406	631	792	1000	1220	1412	1689	1952
	Calif.	pop.	219	219	402	482	576	647	709	829	894	915
# nodes		road	151	170	345	459	572	659	751	872	952	1004
w/ station(s)	Quebec	pop.	28	45	62	99	149	190	206	235	243	256
		road	38	78	105	129	157	175	192	229	242	255
% road nodes	California		85	88	84	81	77	75	64	71	68	68
dual purpose	Quebec		45	63	66	71	68	67	66	51	60	56

dual bound, which might be useful for decision makers to evaluate the quality of the final solution.

We now analyze some characteristics of the solution created by SM for the instances using both Quebec and California networks, with $|T| = 10$. In Fig. 8 we depict the growth of EV adoption over time, for both instances. The superlinear shape of these curves is expected, since the highest values for these adoption rates (4.2% and 6.6% for the Quebec and California instances respectively) are below the inflection point of our proposed growth function ϕ (at 25%).

In Table 6, we present some statistics on the evolution of the charging infrastructure over time. For both instances, we observe that the roll out of charging stations installed within population centers, generally matches the deployment of charging stations along the road network. This can also be observed in the two GIF animations, *quebec.gif* and *california.gif*, provided in the supplementary material, that illustrate per period, the geographic spread of the nodes with at least one charging station. This follows from the problem definition, where the decision of people to adopt EV transportation depends on their ability to charge both along their daily commute and long-haul travels. In both instances, the number of chargers installed along the road network increase over time, relative to those deployed within population centers. We also observe that the average number of chargers per road node with at least one charging station tend to grow over time; the same is not true for nodes representing population centers. This implies that while in the beginning charging stations installed along the road network may only serve a few EV drivers, they are still of great importance since they allow first adopters to complete long-haul travels on their limited-ranged EVs. Finally, in Table 6, we show the percentage of road nodes that have at least one charger that also serves local charging demand. For the California instance, even though this value diminishes over time, it tends to be much larger than for the Quebec instance. This is explained by the topology of both networks: the highway network in California is much more connected with many population centers located along the road, whereas in Quebec's there are large stretches of road without any population center close by.

7. Conclusion

In recent years, many countries have established ambitious goals for EV adoption, in view of reducing greenhouse gas emissions. Nevertheless, the existing EV charging infrastructure remains largely insufficient to service high levels of demand. In this paper, we introduce a new optimization framework for the strategic siting and sizing of fast charging stations for EVs. This framework is based on a multi-period optimization problem, where the charging demand in each period is dynamic, and is influenced by the siting decisions made in previous ones.

To the best of our knowledge, the proposed optimization problem is the first to integrate two types of approaches, node-based and flow based, for the spatial distribution of the EV charging demand. Thereby, we are able to both account for the range limitations of EVs in long-haul travels (likely impossible with a node-based only model), and solve problems for much larger landscapes than the ones that state-of-art flow-based approaches are capable of. For example, two of the largest instances in the literature for flow-based related problems are the California State road network in Yıldız et al. (2016), with 339 candidate locations including 57 population centers, and the DC-NY-BOS network in Zhang et al. (2017) with 317 nodes and 123 population centers; in this paper, we tackle two much larger networks, the Quebec network with 2363 candidate locations including 547 population centers, and the California network with 4608 candidate locations and 1832 population centers.

Another major contribution of our approach is a new evidence-based demand dynamic that is incorporated within the optimization problem. In this dynamic, interest in EV technology follows a contagion-like effect, where the more people see others driving

EVs, the more they contemplate the idea of purchasing an EV themselves. Demand dynamics that have been previously integrated in siting optimization problems do not reflect this social influence (Zhang et al., 2017). The ultimate decision of these potential adopters is based on the availability of charging opportunities, both along their daily commutes and on the way to other farther destinations. By approximating the diffusion of EVs with piecewise linear functions, we are able to model the proposed optimization problem with the MILP formulation described in Section 4.

We solve the aforementioned MILP formulation using a general-purpose MILP solver (CPLEX). In addition, we propose a solution method where we also solve the same formulation, but warm start it with a feasible solution created by the rolling horizon heuristic described in Section 5. In this starting heuristic we solve the same optimization problem on a rolling horizon, i.e., we decompose the problem, so that we solve in succession smaller sub-problems with a single period time horizon, and decisions are carried over to the subsequent iterations. In Section 6, we analyze the results of computational experiments done to evaluate the performance of these solution methods. The results reveal that by warm starting CPLEX with the solution of the rolling horizon heuristic, we are able to efficiently obtain provably good solutions for instances based in the very large siting landscapes mentioned above. We also show that the deployment plans created by the proposed method provide a balanced roll out of charging stations within population centers, which satisfy EV drivers' local charging needs, and along the road network, allowing them to complete long-haul travels without the risk of their EV running out of battery.

In the future, we want to extend the proposed problem to also consider the power availability at the each candidate location, as Level 3 charging stations noticeably affect the load on the electric grid. One idea is to include decisions on the expansion of the power network. In addition, we want to explore ways to model more realistic demand dynamics. In this work, given the same charging availability, the rate of EV adoption is the same for everyone. However, this is not realistic, as people do not all behave in the same fashion. We plan to incorporate choice models in our optimization framework to disaggregate behaviors and preferences for different customer profiles, that account for residence type and/or location, income, and other factors. At the same time, we also want to consider some of these characteristics when modeling the homophily in the contagion networks. In this work, we assumed them to be simply dependent on geographical proximity, but other traits like social reach or socio-demographic similarity (Wolf et al., 2015) can also be included.

Acknowledgments

This research was supported by *Hydro-Québec*, by an Engage Grant from the Natural Sciences and Engineering Research Council (NSERC) of Canada, by the NSERC Energy Storage Technology Network (NESTNet), and by an IVADO Postdoctoral Scholarship. In particular, we gratefully acknowledge the *Électrification des Transports* team at *Hydro-Québec* for sharing with us their expertise on EVs.

Supplementary material

Supplementary material associated with this article can be found, in the online version, at doi:10.1016/j.ejor.2020.01.055.

References

Agency, E. E. (2017a). Greenhouse gas emissions from transport. http://www.eea.europa.eu/data-and-maps/indicators/transport-emissions-of-greenhouse-gases/transport-emissions-of-greenhouse-gases-10.

Anjos, M. F., Gendron, B., & Joyce-Moniz, M. (2019). *Instances for "Increasing electric vehicle adoption through the optimal deployment of fast-charging stations for local and long-distance travel"*. University of Edinburgh, School of Mathematics. doi:10.7488/ds/2746.

Bailey, J., Miele, A., & Axsen, J. (2015). Is awareness of public charging associated with consumer interest in plug-in electric vehicles? *Transportation Research Part D: Transport and Environment, 36*, 1–9. http://www.sciencedirect.com/science/article/pii/S1361920915000103.

Brey, J., Carazo, A., & Brey, R. (2014). Analysis of a hydrogen station roll-out strategy to introduce hydrogen vehicles in andalusia. *International Journal of Hydrogen Energy, 39*(8), 4123–4130. http://www.sciencedirect.com/science/article/pii/S0360319913015863.

Brownstone, D., Bunch, D. S., & Train, K. (2000). Joint mixed logit models of stated and revealed preferences for alternative-fuel vehicles. *Transportation Research Part B: Methodological, 34*, 315–338. http://www.sciencedirect.com/science/article/pii/S0191261599000314.

Bureau, U. S. C. (2018). 2010 United States Census. http://www.census.gov/programs-surveys/decennial-census/decade.2010.html (Consulted on May).

California Air Resources Board (2019). Hydrogen fueling infrastructure assessments, california hydrogen infrastructure tool (CHIT) and california hydrogen accounting tool (CHAT). https://www.arb.ca.gov/msprog/zevprog/hydrogen/h2fueling.htm (consulted on February).

California New Car Dealers Association (2018). California auto outlook: Comprehensive information on the california vehicle market. http://www.cncda.org/wp-content/uploads/California-Covering-1Q-2018.pdf.

Canada, E., & Change, C. (2017). Canadian environmental sustainability indicators: Greenhouse gas emissions. http://www.ec.gc.ca/indicateurs-indicators/18F3BB9C-43A1-491E-9835-76C8DB9DDFA3/GHGEmissions_EN.pdf.

Canada, S. (2018). Canada 2016 census of population. www12.statcan.gc.ca/census-recensement/2016/dp-pd/index-eng.cfm (Consulted on January).

Capar, I., Kuby, M., Leon, V. J., & Tsai, Y. J. (2013). An arc cover-path-cover formulation and strategic analysis of alternative-fuel station locations. *European Journal of Operational Research, 227*, 142–151. http://www.sciencedirect.com/science/article/pii/S0377221712008855.

Carley, S., Krause, R. M., Lane, B. W., & Graham, J. D. (2013). Intent to purchase a plug-in electric vehicle: A survey of early impressions in large US cites. *Transportation Research Part D: Transport and Environment, 18*, 39–45. http://www.sciencedirect.com/science/article/pii/S1361920912001095.

Cavadas, J., de Almeida Correia, G. H., & Gouveia, J. (2015). A MIP model for locating slow-charging stations for electric vehicles in urban areas accounting for driver tours. *Transportation Research Part E: Logistics and Transportation Review, 75*, 188–201. http://www.sciencedirect.com/science/article/pii/S136655451400194X.

Chung, S. H., & Kwon, C. (2015). Multi-period planning for electric car charging station locations: A case of Korean Expressways. *European Journal of Operational Research, 242*, 677–687. http://www.sciencedirect.com/science/article/pii/S0377221714008509.

Circuit électrique. (2018). https://lecircuitelectrique.com/find-a-station (consulted on January).

Dong, J., Liu, C., & Lin, Z. (2014). Charging infrastructure planning for promoting battery electric vehicles: An activity-based approach using multiday travel data. *Transportation Research Part C: Emerging Technologies, 38*, 44–55. http://www.sciencedirect.com/science/article/pii/S0968090X13002283.

Energy, O. o. E. E., & of, R. E. o. t. U. S. D. (2017). Fact of the week #1008: Median all-electric vehicle range grew from 73 miles in model year 2011 to 114 miles in model year 2017. http://www.energy.gov/eere/vehicles/articles/fotw-1008-december-18-2017-median-all-electric-vehicle-range-grew-73-miles.

European alternative fuels observatory. (2018). www.eafo.eu/countries (consulted on May).

Fotheringham, S., & O'Kelly, M. E. (1989). Spatial interaction models: Formulations and applications. In *Vol. 5 of studies in operational regional science*. Kluwer.

Frade, I., Ribeiro, A., Gonçalves, G., & Antunes, A. (2011). Optimal location of charging stations for electric vehicles in a neighborhood in Lisbon, Portugal. *Transportation Research Record: Journal of the Transportation Research Board, 2252*, 91–98.

Guinn, S. (2017). Level 1 vs Level 2 EV charging. http://www.clippercreek.com/level-1-level-2-charging-stations/.

Hong, S., & Kuby, M. (2016). A threshold covering flow-based location model to build a critical mass of alternative-fuel stations. *Journal of Transport Geography, 56*, 128–137.

Hosseini, M., & MirHassani, S. A. (2015). A heuristic algorithm for optimal location of flow-refueling capacitated stations. *International Transactions in Operational Research, 25*, 1377–1403.

Hosseini, M., MirHassani, S. A., & Hooshmand, F. (2017). Deviation-flow refueling location problem with capacitated facilities: Model and algorithm. *Transportation Research Part D: Transport and Environment, 54*, 269–281. http://www.sciencedirect.com/science/article/pii/S1361920916306101.

Huang, Y., Li, S., & Qian, Z. S. (2015). Optimal deployment of alternative fueling stations on transportation networks considering deviation paths. *Networks and Spatial Economics, 15*, 183–204.

Kim, J.-G., & Kuby, M. (2012). The deviation-flow refueling location model for optimizing a network of refueling stations. *International Journal of Hydrogen Energy, 37*, 5406–5420. http://www.sciencedirect.com/science/article/pii/S0360319911020337.

Kim, J.-G., & Kuby, M. (2013). A network transformation heuristic approach for the deviation flow refueling location model. *Computers & Operations Research, 40*, 1122–1131. http://www.sciencedirect.com/science/article/pii/S030505481200247X.

Ko, J., Gim, T.-H. T., & Guensler, R. (2017). Locating refuelling stations for alternative fuel vehicles: a review on models and applications. *Transport Reviews, 37*, 551–570. doi:10.1080/01441647.2016.1273274.

Kuby, M., & Lim, S. (2005). The flow-refueling location problem for alternative-fuel vehicles. *Socio-Economic Planning Sciences, 39*, 125–145. http://www.sciencedirect.com/science/article/pii/S0038012104000175.

Kuby, M., Lines, L., Schultz, R., Xie, Z., Kim, J.-G., & Lim, S. (2009). Optimization of hydrogen stations in florida using the flow-refueling location model. *International Journal of Hydrogen Energy, 34*(15), 6045–6064. http://www.sciencedirect.com/science/article/pii/S0360319909007563.

LeBlanc, L. J., Morlok, E. K., & Pierskalla, W. P. (1975). An efficient approach to solving the road network equilibrium traffic assignment problem. *Transportation Research, 9*, 309–318. http://www.sciencedirect.com/science/article/pii/0041164775900301.

Li, S., & Huang, Y. (2014). Heuristic approaches for the flow-based set covering problem with deviation paths. *Transportation Research Part E: Logistics and Transportation Review, 72*, 144–158. http://www.sciencedirect.com/science/article/pii/S1366554514001860.

Li, S., Huang, Y., & Mason, S. J. (2016). A multi-period optimization model for the deployment of public electric vehicle charging stations on network. *Transportation Research Part C: Emerging Technologies, 65*, 128–143. http://www.sciencedirect.com/science/article/pii/S0968090X16000267.

Lim, S., & Kuby, M. (2010). Heuristic algorithms for siting alternative-fuel stations using the flow-refueling location model. *European Journal of Operational Research, 204*, 51–61. http://www.sciencedirect.com/science/article/pii/S0377221709006717.

Melton, N., Axsen, J., & Goldberg, S. (2017). Evaluating plug-in electric vehicle policies in the context of long-term greenhouse gas reduction goals: Comparing 10 Canadian provinces using the "PEV policy report card". *Energy Policy, 107*, 381–393. http://www.sciencedirect.com/science/article/pii/S030142151730277X.

Mirhassani, S. A., & Ebrazi, R. (2013). A flexible reformulation of the refueling station location problem. *Transportation Science, 47*, 617–628.

Perwoski, J. (2017). How China is raising the bar with aggressive new electric vehicle rules. http://www.forbes.com/sites/jackperkowski/2017/10/10/china-raises-the-bar-with-new-electric-vehicle-rules/#920d3a977acf.

Petroff, A. (2017). These countries want to ban gas and diesel cars. http://money.cnn.com/2017/09/11/autos/countries-banning-diesel-gas-cars/index.html.

Plumer, B. (2016a). It's not just solar panels. Electric cars can be contagious, too. http://www.vox.com/2016/8/29/12690798/electric-cars-contagious.

Plumer, B. (2016b). Solar power is contagious. These maps show how it spreads. http://www.vox.com/2016/5/4/11590396/solar-power-contagious-maps.

Rogers, E. M. (2003). *Diffusion of Innovations* (5th Ed.). Free Press.

Shahraki, N., Cai, H., Turkay, M., & Xu, M. (2015). Optimal locations of electric public charging stations using real world vehicle travel patterns. *Transportation Research Part D: Transport and Environment, 41*, 165–176. http://www.sciencedirect.com/science/article/pii/S1361920915001352.

States, U. (2018). Department of energy. http://www.afdc.energy.gov/fuels/electricity_locations.html#/find/nearest?fuel=ELEC (consulted on May).

Tietge, U., Mock, P., Lutsey, N., & Campestrini, A. (2016). Comparison of leading electric vehicle policy and deployment in Europe. http://www.theicct.org/publications/comparison-leading-electric-vehicle-policy-and-deployment-europe.

Tu, W., Li, Q., Fang, Z., Shaw, S. l., Zhou, B., & Chang, X. (2016). Optimizing the locations of electric taxi charging stations: A spatial temporal demand coverage approach. *Transportation Research Part C: Emerging Technologies, 65*, 172–189. http://www.sciencedirect.com/science/article/pii/S0968090X15003538.

United States Department of Energy's EV Everywhere (2014). Workplace charging challenge, progress update 2014. In *Proceedings of the Employers take charge*.

United States Environmental Protection Agency (2017b). *Inventory of U.S. greenhouse gas emissions and sinks, 1990–2015*.

Upchurch, C., & Kuby, M. (2010). Comparing the p-median and flow-refueling models for locating alternative-fuel stations. *Journal of Transport Geography, 18*, 750–758. http://www.sciencedirect.com/science/article/pii/S0966692310000967.

Upchurch, C., Kuby, M., & Lim, S. (2009). A model for location of capacitated alternative-fuel stations. *Geographical Analysis, 41*, 85–106.

Wang, Y.-W., & Lin, C. C. (2009). Locating road-vehicle refueling stations. *Transportation Research Part E: Logistics and Transportation Review, 45*, 821–829. http://www.sciencedirect.com/science/article/pii/S1366554509000313.

Wang, Y.-W., & Lin, C. C. (2013). Locating multiple types of recharging stations for battery-powered electric vehicle transport. *Transportation Research Part E: Logistics and Transportation Review, 58*, 76–87. http://www.sciencedirect.com/science/article/pii/S1366554513001403.

Wang, Y.-W., & Wang, C. R. (2010). Locating passenger vehicle refueling stations. *Transportation Research Part E: Logistics and Transportation Review, 46*, 791–801. http://www.sciencedirect.com/science/article/pii/S1366554509001513.

Wolf, I., der, T. S., Neumann, J., & de Haan, G. (2015). Changing minds about electric cars: An empirically grounded agent-based modeling approach. *Technological Forecasting and Social Change, 94*, 269–285. http://www.sciencedirect.com/science/article/pii/S0040162514002960.

Woo, J., Choi, H., & Ahn, J. (2017). Well-to-wheel analysis of greenhouse gas emissions for electric vehicles based on electricity generation mix: A global perspective. *Transportation Research Part D: Transport and Environment, 51*, 340–350. http://www.sciencedirect.com/science/article/pii/S1361920916301973.

Xie, F., Liu, C., Li, S., Lin, Z., & Huang, Y. (2018). Long-term strategic planning of inter-city fast charging infrastructure for battery electric vehicles. *Transportation Research Part E: Logistics and Transportation Review, 109*, 261–276. http://www.sciencedirect.com/science/article/pii/S1366554517306294.

Yıldız, B., Arslan, O., & Karaşan, O. E. (2016). A branch and price approach for routing and refueling station location model. *European Journal of Operational Research, 248*, 815–826. http://www.sciencedirect.com/science/article/pii/S0377221715004117.

Zhang, A., Kang, J. E., & Kwon, C. (2017). Incorporating demand dynamics in multi-period capacitated fast-charging location planning for electric vehicles. *Transportation Research Part B: Methodological, 103*, 5–29. http://www.sciencedirect.com/science/article/pii/S0191261516304349.